

A composition-tunable cold atmospheric plasma chip for multiplex-treatment of cells

Fang Wang, Chang Li, Ruotong Zhang, Yuan Liu, Haisong Lin, Lang Nan, Muhammad Ajmal Khan, Yang Xiao, Ho Cheung Shum^{*}, Hui Deng^{*}

Corresponding author: Ho Cheung Shum^{2}, Hui Deng^{1*}

Email:

ashum@hku.hk

dengh@sustech.edu.cn

This PDF file includes:

Figs. S1 to S10

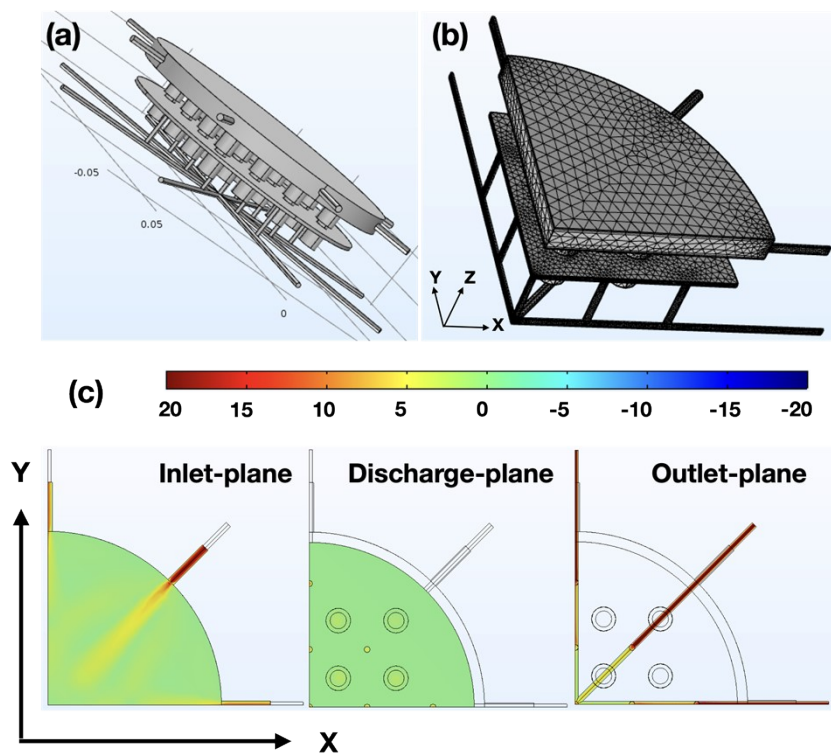


Fig. S1. Gas model and gas flow velocity simulation in COMSOL. (a) The integrated gas model. (b) The meshed model. (One-fourth of the model is computed to simplify the calculation). (c) Feed gas flow velocity in the gas-inlet plane, the discharge plane, and the outlet plane. (The gas flow velocity in the discharge cavity is much less than that in the inlet channels, predicting the reduction of liquid sample surface agitation).



Fig. S2. Graph of the multi-sample holding module. (1) sample-holding array sheet, which also worked as the GE. (2) The glass receptacles. (3) Glass receptacles in the holding wells. (4) Exhaust vents (The surplus gases flow out of the device through those vents).

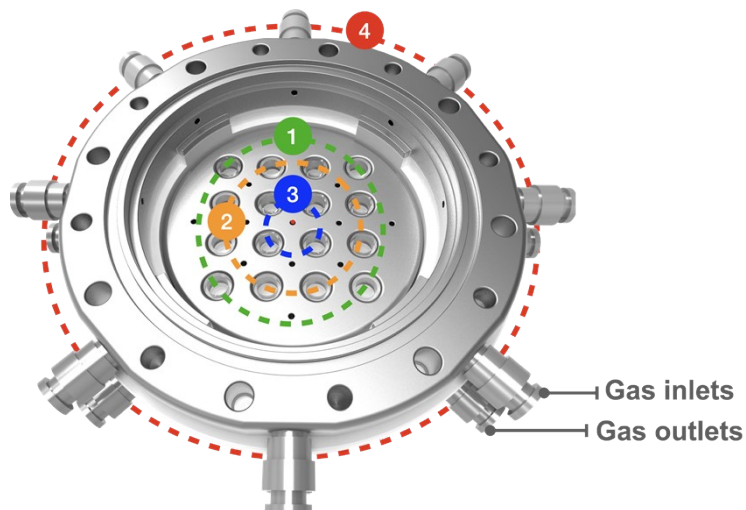


Fig. S3. Graph of the central symmetrically arranged sample-holding wells. (1) The largest concentric circle. **(2)** The medium concentric circle. **(3)** The smallest concentric circle. **(4)** Feed gas inlets situated circle. The wells standing on the three concentric circles bear different distances the center point of the device.

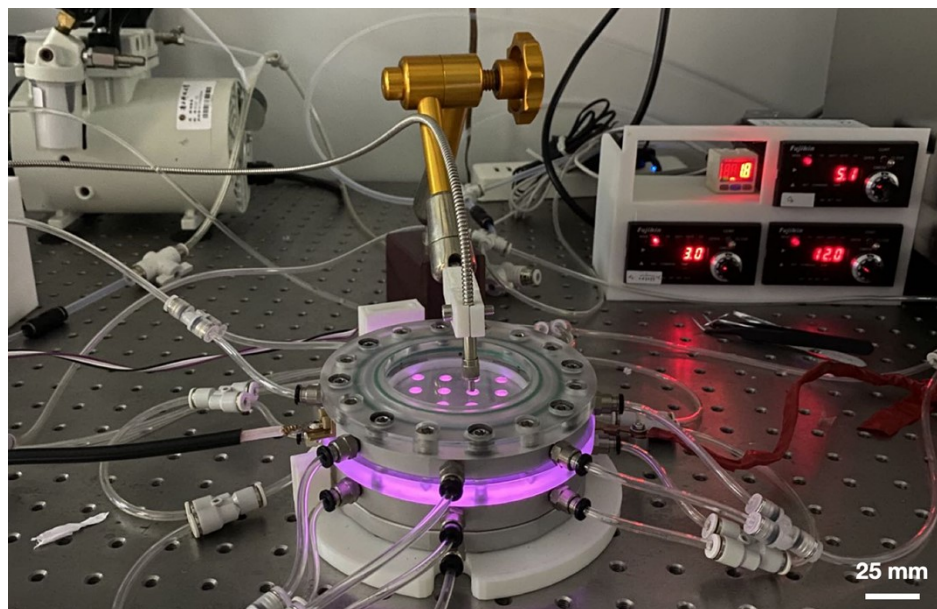


Fig. S4. Graph of the developed cold atmosphere plasma chip in working station
(helium and nitrogen mixture as source gas).

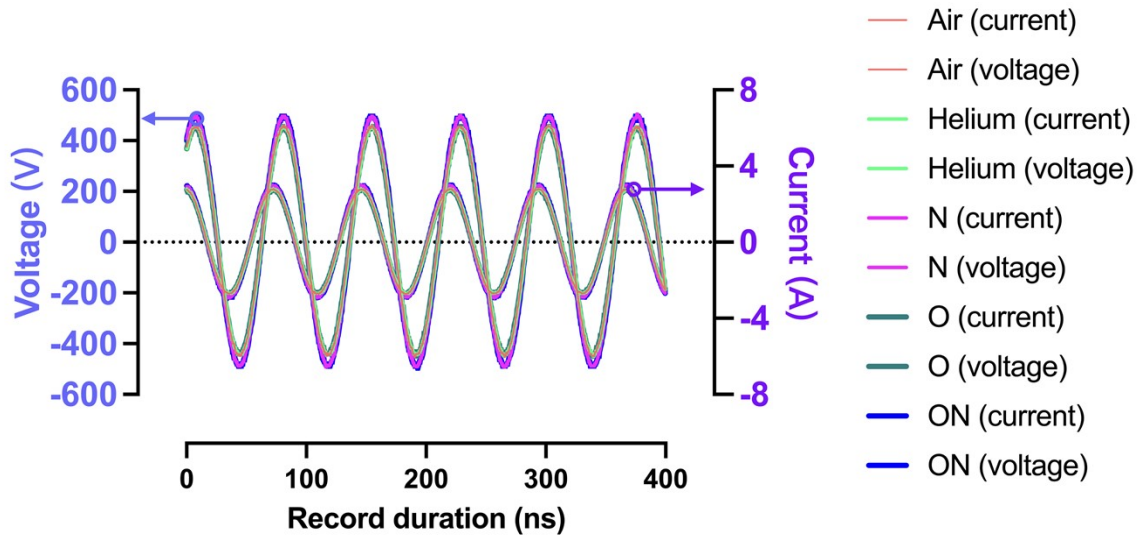


Fig. S5. The current-voltage waveforms when plasmas were ignited with 100 mL DMEM in the receptacles. The waveforms transformed periodically. The amplitude values approached a constant value.

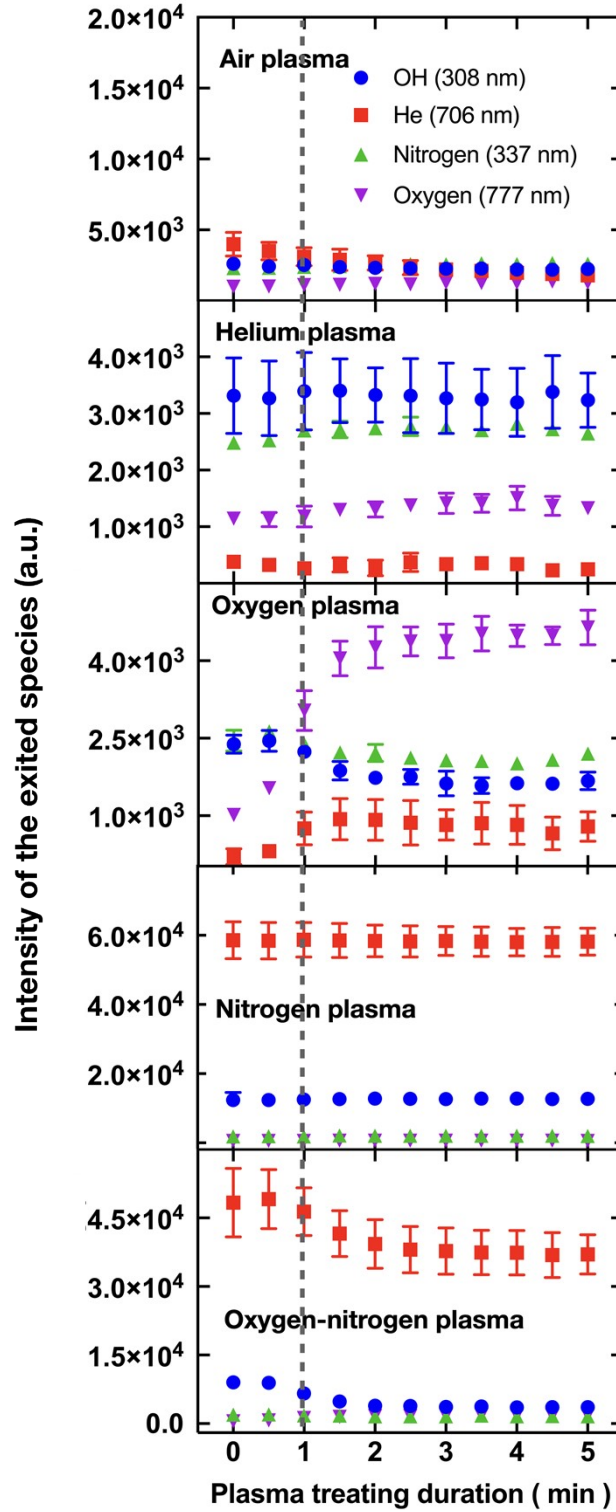


Fig. S6. Intensity evolution of all observed species in the five plasmas.

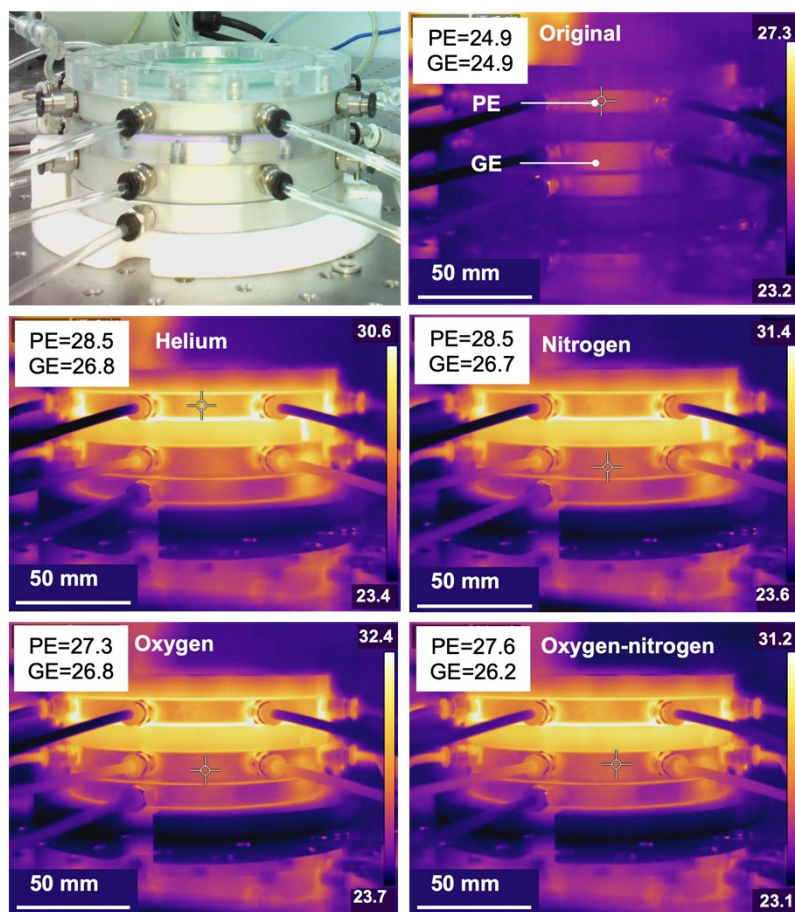


Fig. S7. Graph of temperature increases of the electrodes after 5 min treatment with 100 mL DMEM in the receptacles. The temperature increase of PE is a little higher than GE, which is due to the function of the cooling system embedded at the bottom of GE.

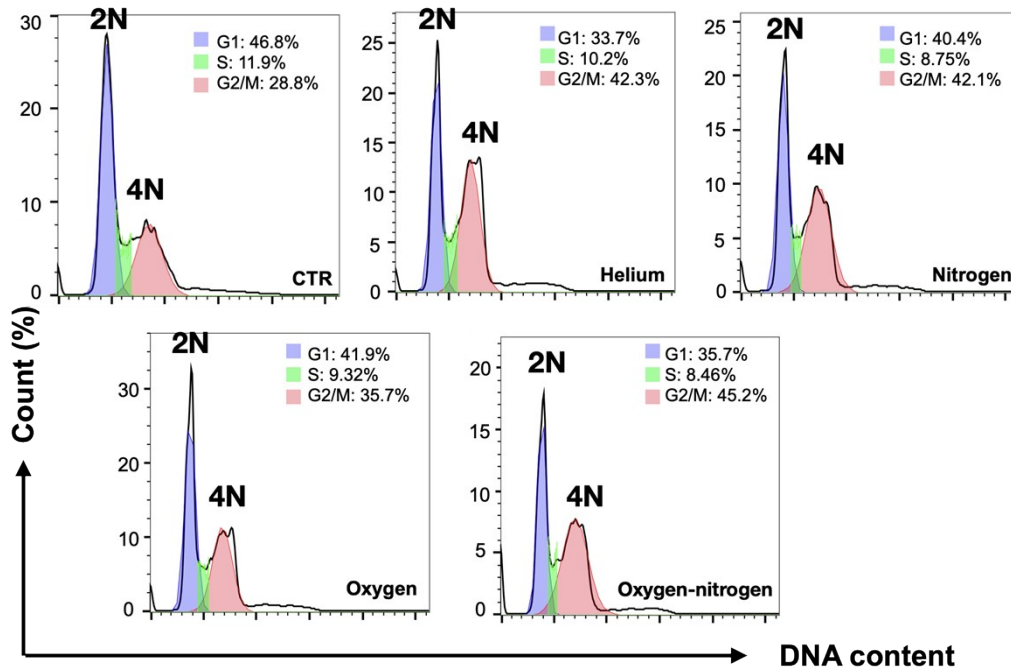


Fig. S8. The cell cycle distribution of HepG2 cells after the treatment of different plasmas for 5 min. (2N means diploid, 4N means tetraploid). DNA content in G2/M phase cells is two times higher than cells in the G0/G1 phase, whereas DNA content in the S phase is between the other two phases as the cells are experiencing the DNA synthesis process. DNA could be linked with the fluorescence dye of PI. In our work, cell cycle distribution was identified by labeling DNA content with fluorescence dye PI.

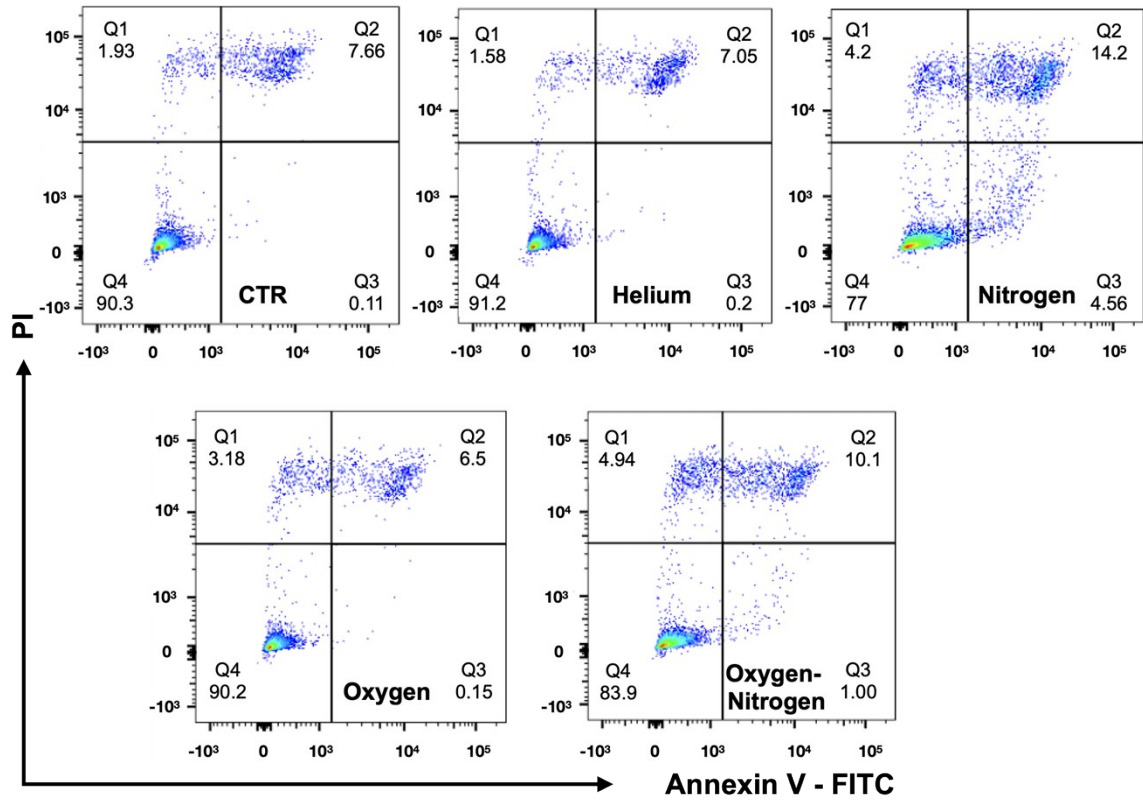


Fig S9. The apoptotic death of HepG2 cells after the treatment of different plasmas for 5 min. At early apoptosis, serine will transfer from the inner layer to the outer layer cell membrane. Thus, early apoptotic cells can be stained by fluorescence dye linked with annexin V which could combine with serine. At late apoptosis, the cell membrane integrity was broken, leaving the fluorescence dye of PI easily to get into the cells to stain the DNA. In our work, suspension cells are stained both by FITC and PI to illustrate cell apoptosis conditions.

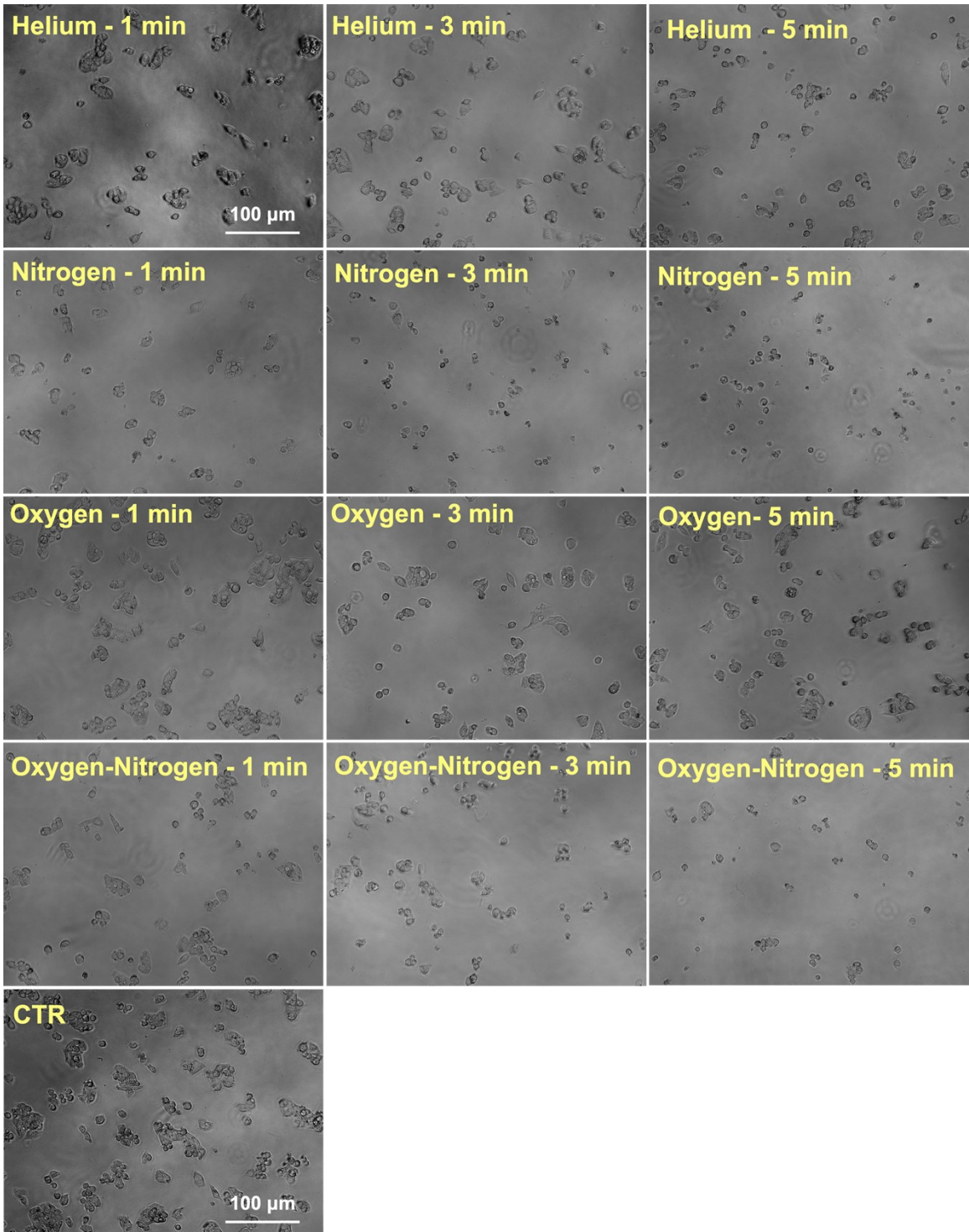


Fig. S10. Microscope graph of HepG2 cells treated with different types of plasmas for 1, 3, and 5min after 24 hours of incubation (The scale bar for all the pictures is same).